

Design techniques for superposition of acoustic bandgaps using fractal geometries

S. Castiñeira-Ibáñez

Dpto. Física Aplicada, Universidad Politécnica de Valencia.

V. Romero-García and J.V. Sánchez-Pérez*

*Centro de Tecnologías Físicas: Acústica,
Materiales y Astrofísica, Universidad Politécnica de Valencia.*

L.M. Garcia-Raffi

*Instituto Universitario de Matemática Pura y Aplicada,
Universidad Politécnica de Valencia.*

(Dated: June 18, 2018)

Abstract

Research into properties of heterogeneous artificial materials, consisting of arrangements of rigid scatterers embedded in a medium with different elastic properties, has been intense throughout last two decades. The capability to prevent the transmission of waves in predetermined bands of frequencies -called bandgaps- becomes one of the most interesting properties of these systems, and leads to the possibility of designing devices to control wave propagation. The underlying physical mechanism is destructive Bragg interference. Here we show a technique that enables the creation of a wide bandgap in these materials, based on fractal geometries. We have focused our work in the acoustic case where these materials are called Phononic/Sonic Crystals (SC) but, the technique could be applied any types of crystals and wave types in ranges of frequencies where the physics of the process is linear.

PACS numbers: 43.20.+g, 43.35.+d

Research into properties of heterogeneous artificial materials, consisting of arrangements of rigid scatterers embedded in a medium with different elastic properties, has been intense throughout last two decades. The capability to prevent the transmission of waves in predetermined bands of frequencies -called bandgaps- becomes one of the most interesting properties of these systems, and leads to the possibility of designing devices to control wave propagation. The underlying physical mechanism is destructive Bragg interference. Here we show a technique that enables the creation of a wide bandgap in these materials, based on fractal geometries. We have focused our work in the acoustic case where these materials are called Phononic/Sonic Crystals[1, 2] (SC) but, the technique could be applied any types of crystals and wave types in ranges of frequencies where the physics of the process is linear.

If we consider acoustically-hard cylinders (scatterers) periodically embedded in air (host), then the difference between velocities and densities in the scatterers and embedding medium are very large. So the physical problem is reduced to that of array scattering based on Bragg's law. With these conditions, the position and the size of the bandgaps in the range of frequencies depend on: a) the arrangement of the scatterers, according to the Bragg law and b) the amount of matter formed by the scatterers, quantified by the filling fraction (ff). For a given SC, an increase in the bandgaps can be obtained only by an increasing the ff. There are two main ways for varying the characteristics of full SC bandgaps[3, 4]. First, by varying the acoustical properties of the scatterers[5–7] or, secondly, by developing new arrangements of scatterers with further crystalline symmetries. Quasi crystals[8] and Quasi Ordered Structures[9] are examples of this second strategy. Also, other authors [10] have developed an optimized design technique that could be applied to the case of elastic/acoustic waves, based on the concept of hyperuniformity, to obtain large and complete bandgaps with amorphous photonic materials. Here, we propose a new way to obtain large bandgaps based on the redistribution of the elements of the SC based on fractal geometries[11]. We have chosen these geometries because they can be modelled mathematically and they can be used as design tools. Recently fractals have been under study for a wide range of practical applications, from biological or medical[12] to economics[13]. In fact, fractals have been used for SCs[14–17] but only to design of the shapes of the scatterers[18].

As the first step we have designed an arrangement of scatterers inside an equilateral triangle of side L , based on a 2D fractal called Sierpinsky triangle (see figure 1). We have chosen a 2D symmetry triangular pattern that presents the highest bandgap as a consequence

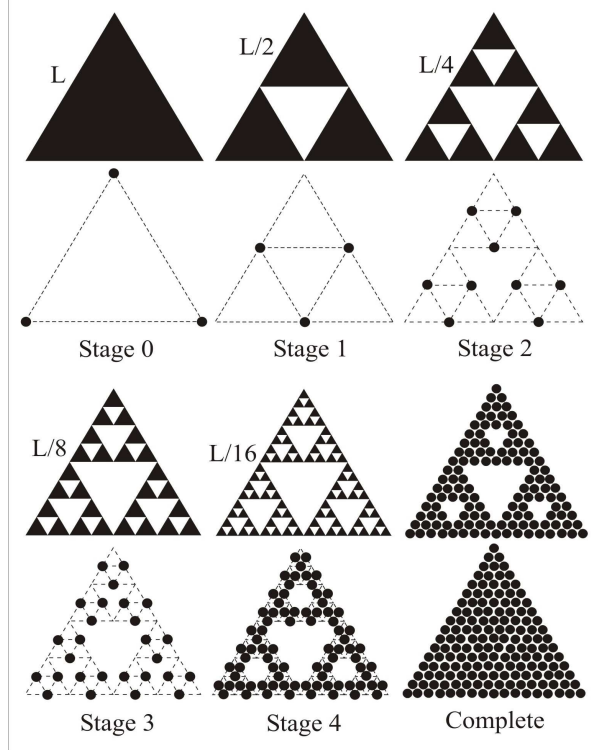


FIG. 1. Quasi fractal arrangement of scatterers: Five stages of cylinder arrays based on the Sierpinski's triangle geometry and the resulting complete structure.

of its degree of hyperuniformity[10]. In this figure, we represent a transversal section (in the XY plane) of our arrangement assuming infinitely long cylinders with radius r parallel to the z axis. We have called it Quasi Fractal Structure (QFS) because, although the fractal construction follows an infinite iterative process[11], we only show here the first five iterations to take account of the space restrictions given by both L and r . Figure 1 shows also that a cylinder is located at every vertex of the empty triangles in each stage, except stage zero where we have located the scatterers at the vertex of the existing triangle. Also, figure 1 shows the sum of the different stages of our fractal arrangement (complete figure). At first glance one might think that it is a classical triangular crystalline array with some vacancies in its structure. However, the underlying symmetry follows a fractal pattern. Thus, we can consider the complete figure as a sum of independent triangular arrays with different lattice constants (L , $L/2$, $L/4$, $L/8$ and $L/16$), with every stage located iteratively within the previous one. This provides a compact small device and the obtained resultant full bandgap results from the sum of the Bragg peak corresponding to every array. This idea is consistent

with the nature of fractal geometries based as they are on the repetition of identical motifs at differing size scales[11].

Another argument to explain the existence of a large full bandgaps is related to the relationship among the different lattice constants. Here they are proportional to $1/2^M$, being M the order number of the stage. This produces a repetition of many Bragg peaks at different stages and a reinforcement of the bandgap. It is possible to find an expression to obtain the number of repeated Bragg peaks at different stages. The following functions $S_\alpha(n, M)$, $\alpha = 0^\circ, 30^\circ$ give the value of the frequency for which the n -th Bragg peak appears at the different stages M ($M = 0, 1, 2, 3, 4$), as a function of L and along the two high-symmetry directions of the triangular array ($0^\circ, 30^\circ$)

$$\begin{aligned} S_{0^\circ}(n, M) &= C_{0^\circ}(n+1)2^M; \\ S_{30^\circ}(n, M) &= C_{30^\circ}(n+2)2^{M-1}, \end{aligned} \tag{1}$$

where $C_{0^\circ} = \sqrt{3}/3$ and $C_{30^\circ} = 2/3$ due to the Bragg law. Based on expressions (1), it is straightforward to find the relationship of appearance of a predetermined Bragg peak for any two different stages

$$\begin{aligned} (0^\circ) \quad n &= (n' + 1)2^V - 1; \\ (30^\circ) \quad n &= (n' + 2)2^V - 2, \end{aligned} \tag{2}$$

where V is the difference between the couple of stages we want to compare ($V = 1, 2, 3, 4$). Equations (2) show the relationship between the n -position of appearance of a Bragg peak in the stage M as a function of the n' position of appearance of the same peak in another stage M' , such that $V = M' - M$. Note the large number of times certain Bragg peaks are repeated on different stages according with (2), producing an reinforcement and, as a consequence, an enhancement of the full bandgap.

The second, and much more important, step of our design technique consists in varying the diameter of each set of cylinders for each stage independently. Thus, the scatterers are distributed in a more efficient way, increasing the sizes in the large stages and reducing them in the others, thereby providing each stage with the adequate value of ff for the appearance

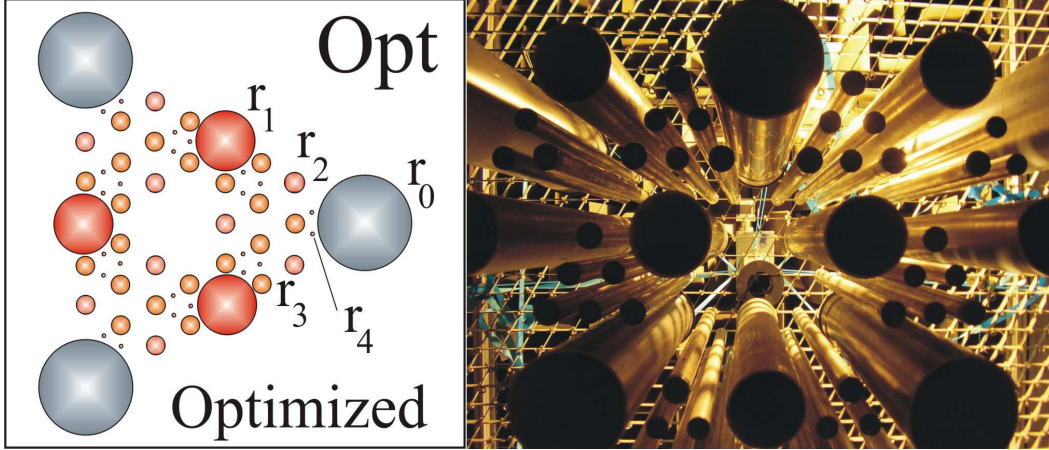


FIG. 2. (Left) Optimized arrangement of scatterers based on Sierpinski triangle with different relationships among the radii of the cylinders (QFS_{Opt}); (Right) Photograph taken from beneath the commercial arrangement (QFS_{Exp}) used to validate theoretical results. Part of the supporting frame can be seen also.

of their Bragg's peaks. As a consequence, a further increase of the full bandgap occurs. In figure 2 we show a proposed QFS built with an optimized relationship between the radii of the cylinders belonging to the different stages M ($M = 0, 1, 2, 3, 4$). For the optimization process we have used genetic algorithm already adapted to the acoustic case[9] (QFS_{Opt}) ($r_0/L \approx 0.14$; $r_1/L \approx 0.09$; $r_2/L \approx 0.03$; $r_3/L \approx 0.032$; $r_4/L \approx 0.02$). Note that it has been necessary to remove some cylinders of the starting complete array shown in figure 1 in order to place the biggest cylinders (large radii) of first stages. Of course, other relationships among the radii of the cylinders could be appropriate other applications.

To quantify the size of the bandgap of this device we have used the Attenuation Area parameter[9] (AA) in the analyzed range of frequencies and, at the moment, only along the ΓX direction (0° of incidence on the sample). Comparing the AA value for the QFS_{Opt} designed with the corresponding to a classical SC with triangular array constructing with the same external size and shape and with cylinder radius $r/L \approx 0.02$, we obtain interesting results: AA parameter grows, in QFS_{Opt} case ($AA_{Opt}=179.88$ normalized units) more than 400% compared with the classical triangular lattice ($AA_{SC}=43.94$ n.u.). But keep in mind that QFS_{Opt} has been designed under the premise of maintaining the same ff as SC by means of genetic algorithms ($ff_{Opt}=ff_{SC}=36\%$). With these data, we can break the rule about the relationship between ff and the size of the bandgaps: we have obtained a high increase in the

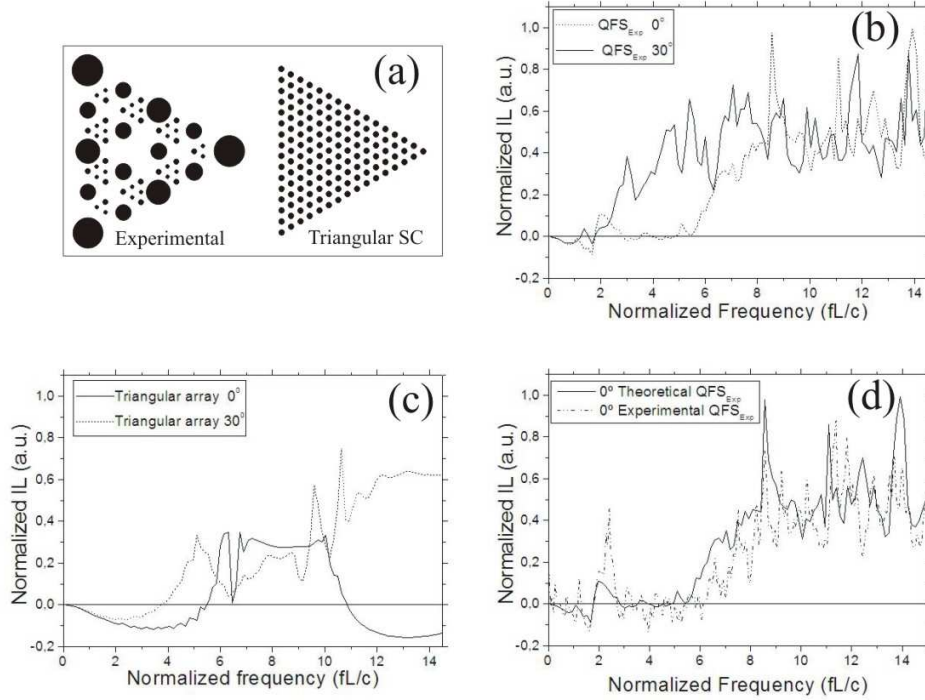


FIG. 3. Non-transmission properties of the designed devices: (a) Experimental Quasi Fractal Structure (QFS_{Exp}) and the triangular SC used. The relationship among the radii of the cylinders for the first case is ($r_0/L \approx 0.094$; $r_1/L \approx 0.078$; $r_2/L \approx 0.054$; $r_3/L \approx 0.029$; $r_4/L \approx 0.017$), being ($ff_{Exp}=33\%$); (b) Theoretical normalized IL spectra along the two high-symmetry directions for QFS_{Exp}. (c) The same for the triangular array ($ff_{SC}=36\%$); (d) Both Theoretical and Experimental QFS_{Exp} attenuation spectra for ΓX direction.

size of the bandgap without increasing the ff of the device in respect of the original triangular array device. These results have been calculated in the normalized range of frequencies 0-15 shown in figure 3. Moreover, due to the nature of our technique, the crystal wave properties of our device remain intact for each stage as it is a sum of triangular arrays. This means that both the bandgap obtained along the other high-symmetry direction ΓJ (30°) and the full bandgap also grow (200% in the case of the full bandgap).

To illustrate the above statement experimentally we have constructed a new device similar to QFS_{Opt} but with commercially available hollow cylinders, QFS_{Exp} (figure 3a). In figures 3b-3c one can compare the theoretical normalized insertion loss spectra (IL), along the two high-symmetry directions ΓX and ΓJ (0° - 30°), for both QFS_{Exp} and the SC defined above.

We have used Multiple Scattering Theory[19, 20] to obtain these spectra, which have been calculated at a distance $d = 1/L$ from the edge of the samples. Also, in figure 3d we show the good agreement between the theoretical and experimental results for 0° incidence.

In summary, in this work we have shown that an optimised fractal-based design technique enables a large increase of the scattering bandgaps for sonic crystal arrays if rigid scatterers. There are two steps. The first consists of the use of fractal patterns to arrange the scatterers. The resulting device is the sum of several independent crystalline arrays. The second step consists of optimising the nested arrays by varying the ff of each fractal stage independently. As a result, we have obtained efficient and compact devices. The sum of the Bragg peaks belonging to the different scale arrays (stages), the reinforcement process due to the existence of different lattice constants and the redistribution of cylinders among the different stages are behind this enhancement.

This work was supported by MCI (Spanish Government) and FEDER funds, under Grant Nos. MAT2009-09438 and MTM2009-14483-C02-02. The authors would like to thank Prof. K. Attenborough and Dr. E.A. Sánchez-Pérez for their suggestions and for the revision of the manuscript.

* jusanc@fis.upv.es

- [1] R. Martínez-Sala, J. Sancho, J. V. Sánchez, V. Gómez, J. Llinares, and F. Meseguer, *nature* **378**, 241 (1995).
- [2] J. V. Sánchez-Pérez, D. Caballero, R. Martínez-Sala, C. Rubio, J. Sánchez-Dehesa, F. Meseguer, J. Llinares, and F. Gálvez, *Phys. Rev. Lett.* **80**, 5325 (1998).
- [3] A. Khelif, M. Wilm, V. Laude, S. Ballandras, and B. Djafari-Rouhani, *Phys. Rev. E* **69**, 067601 (2004).
- [4] J. Sánchez-Pérez, C. Rubio, R. Martínez-Sala, R. Sánchez-Grandia, and V. Gómez, *Appl. Phys. Lett.* **81**, 5240 (2002).
- [5] O. Umnova, K. Attenborough, and C. M. Linton, *J. Acoust. Soc. Am.* **119** (2006).
- [6] Z. Liu, X. Zhang, Y. Mao, Y. Zhu, Z. Yang, C. Chan, and P. Sheng, *Science* **289**, 1734 (2000).
- [7] W. Kuang, Z. Hou, and Y. Liu, *Phys. Lett. A* **332**, 481 (2004).
- [8] X. Zhang, *Phys. Rev. B* **75**, 024209 (2007).

- [9] V. Romero-García, E. Fuster, L. M. García-Raffi, E. A. Sánchez-Pérez, M. Sopena, J. Llinares, and J. V. Sánchez-Pérez, *Appl. Phys. Lett.* **88**, 174104 (2006).
- [10] M. Florescu, S. Torquato, and P. Steindhardt, *PNAS* **106**, 2009 (20658-20663).
- [11] B. Mandelbrot, *The fractal geometry of the nature* (W.H. Freeman & Co., New York,, 1983).
- [12] P. Iannaccone and I. . Khokha, M. CRC Press, *Fractal Geometry in Biological Systems: An Analytical Approach.* (CRC Press, Inc., 1996).
- [13] B. Williams and B. Trading, *Chaos: Applying Expert Techniques to Maximize Your Profits* (Market place Books, Inc., 1995).
- [14] F. Frezza, L. Pajewski, and G. Schettini, *IEEE Trans. Microwave Theory Tech.* **52**, 220 (2004).
- [15] L. Liang, *Chin. Phys. Lett.* **20**, 1767 (2003).
- [16] Y. Fu, N. Yuan, and G. Zhang, *Microwave Opt. Technol. Lett.* **136-138**, 2002 (32).
- [17] L. Zheng, X. Jian-Jun, and L. Zhi-Fang, *Chin. Phys. Lett* **20**, 516 (2003).
- [18] R. Norris, J. S. Hamel, and P. Nadeau, *J. Appl. Phys.* **104908**, 2008 (103).
- [19] Y.-Y. Chen and Z. Ye, *Phys. Rev. E* **64**, 036616 (2001).
- [20] D. García-Pablos, M. Sigalas, F. M. de Espinosa, M. Torres, M. Kafesaki, and N. García, *Phys. Rev. Lett.* **84**, 4349 (2000).